04

Breakdown mechanism of a high-frequency discharge with jet electrolytic electrodes

© V.S. Zheltukhin[1], Al.F. Gaisin[2], S.Y. Petryakov[1]

[1] Tupolev Kazan National Research Technical University (KAI), Kazan, Tatarstan, Russia
[2] Joint Institute for High Temperatures, Russian Academy of Sciences, Moscow, Russia
E-mail: almaz87@mail.ru

Received April 27, 2022
Revised July 16, 2022
Accepted July 18, 2022

The physical mechanism for the emergence of ring and semi-ring plasma structures around electrolyte jets in a high-frequency discharge with liquid jet electrodes. It is shown that the electric field strength in the jet flow decay region can reach values of 10^9-10^{10} V/m, at which autoelectronic emission is possible, leading to the appearance in the vicinity of the jet of primary electrons, which leads to ionization and excitation of the molecules of the surrounding gaseous medium.

Keywords: Plasma-liquid systems, high-frequency discharge, electrolytes, numerical methods.

DOI: 10.21883/TPL.2022.09.55076.19237

Plasma-liquid systems are a part of a surging interdisciplinary research field that encompasses gas discharge physics, fluid and gas dynamics, thermodynamics, chemistry of multiphase systems, and plasma chemistry [1]. One or both of the electrodes in such systems are electrolytic with alternating or direct current supplied to them. If both electrodes are electrolytic, one or two of them are flow-type [2]. The interest in plasma-liquid systems stems in no small part from their application potential (e.g., in processing of metal surfaces [3], production of fine powders [4], water and air purification [5], etc.).

The results of experimental examination of a high-frequency (HF) discharge between two jet electrolytic electrodes under an ambient atmospheric pressure ranging from 10^3 to 10^5 Pa have been presented in our earlier studies [6,7]. Various glowing ring or semi-ring structures forming in the jet flow decay region were observed in these experiments. At the same time, the mechanism of formation of ring plasma structures remained unexamined.

The aim of the present study is to establish the mechanism of formation of ring plasma structures based on the obtained experimental and numerical data.

It is known that free (primary) charged particles and an electric field, which induces their directed motion, are needed to initiate a breakdown [8]. In a gas discharge between metallic electrodes, the emission of electrons from the cathode surface or the ionization of gas under the influence of natural radioactivity and cosmic radiation are the sources of primary electrons. An electrolyte differs from a metal in that it has no free electrons; charged particles in electrolytes are negative or positive ions. Spontaneous ionization under the influence of natural radioactivity or cosmic radiation is also of little importance in this case, since a discharge is often produced in jet decay even before the moment of droplet detachment [6]. Therefore, the electric field induced by the jet current is examined in order to determine the mechanism of emergence of glowing structures and jet breakdown under a discharge between two electrolytic electrodes.

Let us assume that an electrolyte jet freely outflowing vertically from a feeding device is symmetric with respect to the flow axis. The cross section of this jet decreases with distance from the source; thus, its profile is a truncated cone that passes smoothly into a sinusoid with a decreasing amplitude. The radius of the jet cross section at the source is 2.5 mm, and the maximum amplitude of the sinusoid profile

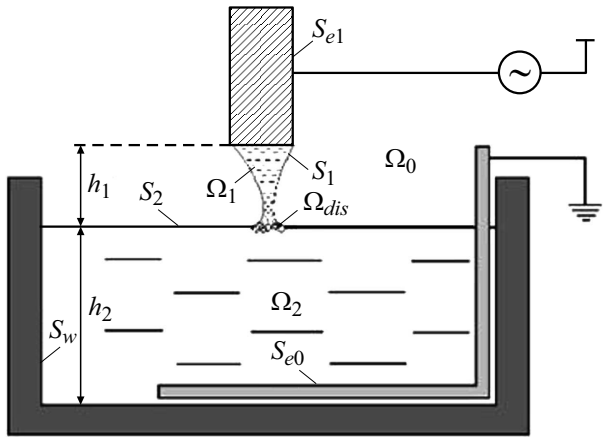

Figure 1. Diagram of regions of a discharge with electrolytic electrodes. Ω_0 is the region occupied by gas, Ω_1 is the region occupied by an electrolytic electrode, Ω_2 is the region of an electrolytic electrode in an electrolytic bath, Ω_{dis} is the gas-vapor discharge region, S_{e0} is the grounded electrode surface, S_{e1} is the feeding tube surface, S_1 is the free jet surface, S_2 is the free surface of liquid in the electrolytic bath, S_w is the surface of walls of the electrolytic bath, h_1 is the jet length, and h_2 is the electrolytic bath depth.

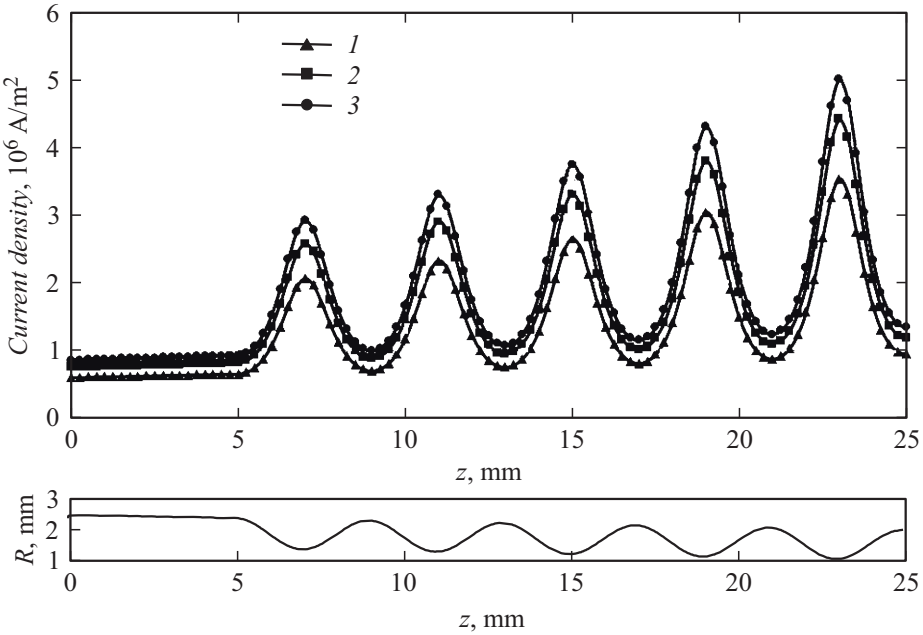

Figure 2. Current density in a jet at current $I = 12$ (*1*), 15 (*2*), and 17 A (*3*). The jet electrode profile is shown below.

at the jet end is 2.0 mm; the point of transition between the cone and the sinusoid profile is located at distance $z = 5$ mm from the source. The sinusoid period is 5 mm. This is an approximation of the actual profile of the jet electrode used in experiments (Fig. 1) [6,7].

Let us introduce local coordinate system $Oxyz$ with its origin being located at the center of the exit aperture of the feeding tube and the positive direction of axis Oz being aligned with the flow direction. HF current $\tilde{I} = I_m \exp(i\omega t)$, where, in accordance with the results of earlier experimental studies [7], amplitude $I_m = 12{-}17$ A, is supplied to the feeding tube.

Alternating current $\tilde{\mathbf{j}} = (0, 0, \tilde{j}_z) \sim \exp(i\omega t)$, which flows along the Oz direction, induces an electromagnetic field with components $\tilde{\mathbf{B}}=(0, \tilde{B}_\varphi, 0)\sim \exp(i\omega t)$ and $\tilde{\mathbf{E}} = (\tilde{E}_r, 0, \tilde{E}_z) \sim \exp(i\omega t)$, where $\tilde{\mathbf{B}}$, $\tilde{\mathbf{E}}$ are the magnetic and electric vectors, $\omega = 2\pi f$ is the circular frequency, f is the current frequency, and i is an imaginary unit ($i^2 = -1$). If I_m, $j_{m,z}$ are the amplitude values of current and current density, respectively, and $r_c = r_c(z)$ is the current jet radius,

$$j_{m,z}(z) = I_m/\pi r_c^2(z). \tag{1}$$

It follows from formula (1) that the current density in a narrowing jet increases in inverse proportion to the radius (Fig. 2). At current $I_m = 12{-}17$ A, the current density amplitude in the jet is as high as $j_{m,z} \sim 10^6$ A/m^2.

Let us introduce magnetic vector potential $\tilde{\mathbf{A}}$ such that $\tilde{\mathbf{B}} = \nabla \times \tilde{\mathbf{A}}$. Inserting it into Maxwell equations

$$\nabla \times \tilde{\mathbf{H}} = \tilde{\mathbf{j}} + \frac{\partial \tilde{\mathbf{D}}}{\partial t}, \qquad \nabla \times \tilde{\mathbf{E}} = -\frac{\partial \tilde{\mathbf{B}}}{\partial t}, \tag{2}$$

$$\nabla \cdot \tilde{\mathbf{B}} = 0, \qquad \nabla \cdot \tilde{\mathbf{D}} = 0, \tag{3}$$

$$\tilde{\mathbf{B}} = \mu_0 \tilde{\mathbf{H}}, \qquad \tilde{\mathbf{D}} = \varepsilon_0 \tilde{\mathbf{E}} \tag{4}$$

and applying the complex amplitude method [9], we obtain

$$\nabla \times \tilde{\mathbf{E}} = -\frac{\partial \tilde{\mathbf{B}}}{\partial t} = -i\omega \mathbf{B}_A \exp(i\omega t) = -i\omega \tilde{\mathbf{B}}, \tag{5}$$

where $\mathbf{B}_A$ is the complex-amplitude vector, $\tilde{\mathbf{B}} = \mathbf{B}_A \exp(i\omega t)$. It follows that

$$\tilde{\mathbf{B}} = \frac{i}{\omega} \nabla \times \tilde{\mathbf{E}} = \nabla \times \tilde{\mathbf{A}}. \tag{6}$$

Thus, $\tilde{\mathbf{E}} = -i\omega \tilde{\mathbf{A}}$.

Let us introduce vectors of complex amplitudes $\mathbf{j}_m$, $\mathbf{H}_m$, $\mathbf{E}_m$, and $\mathbf{A}_m$ given by

$$\tilde{\mathbf{j}} = \mathbf{j}_m \exp(i\omega t), \qquad \tilde{\mathbf{H}} = \mathbf{H}_m \exp(i\omega t),$$
$$\tilde{\mathbf{E}} = \mathbf{E}_m \exp(i\omega t), \qquad \tilde{\mathbf{A}} = \mathbf{A}_m \exp(i\omega t). \tag{7}$$

The following relations hold true for the complex-amplitude vectors:

$$\nabla \times \mathbf{H}_m = \mathbf{j}_m + i\varepsilon_0 \varepsilon \omega \mathbf{E}_m,$$
$$\nabla \times \mathbf{E}_m = -i\mu_0 \omega \mathbf{H}_m, \quad \mathbf{E}_m = -i\omega \mathbf{A}_m. \tag{8}$$

Applying the Biot–Savart law to complex amplitudes, we find

$$\mathbf{E}_m(\mathbf{r}_0) = -i\omega \mathbf{A}_m(\mathbf{r}_0) = -i\omega \frac{\mu_0}{4\pi} \int \frac{\mathbf{j}_m(\mathbf{r}) dV}{|\mathbf{r}_0 - \mathbf{r}|}. \tag{9}$$

Here, $\mathbf{r}_0$ and $\mathbf{r}$ are radius vectors. Combining dependence (1) with Eq. (9), we find that the real amplitude components of the complex electric intensity at the jet boundary are

$$\mathrm{Re}E_{m,r}(r_c, z) = \frac{I_m \omega}{2\pi \varepsilon_0 r_c^2(z)} \frac{\partial r_c}{\partial z},$$
$$\mathrm{Re}E_{m,z}(r_c, z) = -\frac{I_m \omega}{\pi \varepsilon_0 r_c^2(z)}. \tag{10}$$

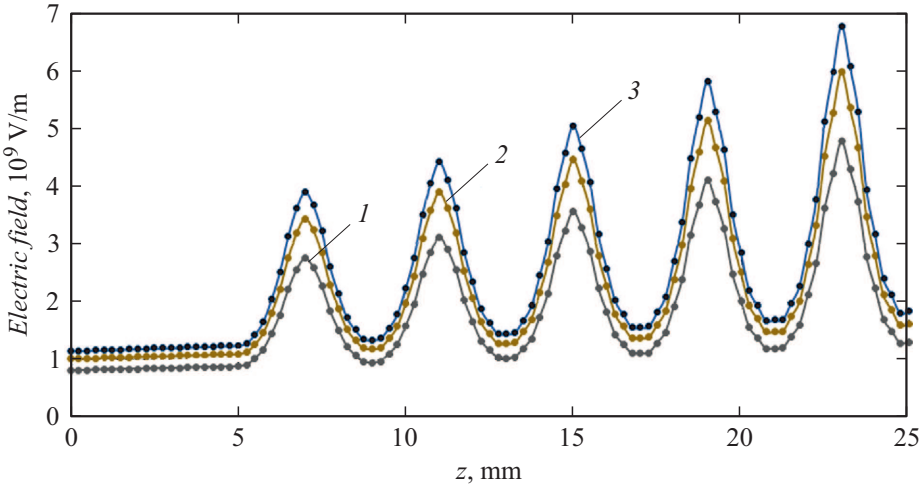

Figure 3. Electric field intensity $\mathrm{Re}E_{m,z}$ at current $I = 12$ (*1*), 15 (*2*), and 17 A (*3*).

The results of calculations revealed that the electric field intensity on the jet surface reaches its maximum of $\geqslant 10^9$ V/m at local minima of the flow radius (Fig. 3). The tunnel effect, which induces the emission of electrons from negatively charged ions at the jet surface, is feasible in an electric field of this intensity [10] and appears to be the most probable cause of emergence of primary electrons. This leads to subsequent breakdown in the regions of decay of a jet and its transition to dripping flow and to the emergence of ring and semi-ring diffuse plasma structures.

The narrowing of a jet in the decay region translates into a quadratic increase in the current density and subsequent heating of this jet to the boiling point, which is what is observed in experiments [6,7,11]. A gas-vapor bubble forms in this case, the flow is interrupted, and the jet resistance increases sharply, inducing voltage (up to 10–20 kV) and current (up to 10–20 A) jumps.

The effect of discharge ignition at different points within a jet and the existence of different plasma formations reported in [6,7] are attributable to the interaction of Tonks–Frenkel and Rayleigh–Taylor instabilities [12], which evolve in liquids in an electric field and in accelerated liquids (vertically outflowing jets), respectively.

The calculation of intensity of the electric field induced by the current flowing along an electrolyte jet in a discharge between two electrolytic electrodes showed that the electric field intensity in jet decay regions is as high as $\mathrm{Re}E_{m,z} \geqslant 10^9$ V/m, while the current density reaches a maximum of $j_{m,z} \geqslant 10^6$ V/m^2. The jet is heated to the boiling point at current antinodes; this results in the formation of a gas-vapor region. Free electrons are produced as a result of autoelectronic emission (tunnel effect) under the influence of the electric field in the regions of jet constriction and in the gas-vapor region. This leads to breakdown of the gas-vapor region and the emergence of ring and semi-ring plasma structures.

Thus, the obtained numerical data agree qualitatively with the results of experiments and the current concepts of interaction between the electric field and materials.

Funding

This study was supported financially by the Russian Science Foundation (project No. 21-79-30062).

Conflict of interest

The authors declare that they have no conflict of interest.

References

[1] P.J. Bruggeman, A. Bogaerts, J.M. Pouvesle, E. Robert, E.J. Szili, J. Appl. Phys., **130** (20), 200401 (2021). DOI: 10.1063/5.0078076
[2] N.F. Kashapov, R.N. Kashapov, L.N. Kashapov, J. Phys. D: Appl. Phys., **51** (49), 494003 (2018). DOI: 10.1088/1361-6463/aae334
[3] A.F. Gaysin, A.K. Gilmutdinov, Inorg. Mater. Appl. Res., **12** (3), 633 (2021). DOI: 10.1134/S2075113321030102
[4] T.A. Kareem, A.A. Kaliani, Ionics, **18** (3), 315 (2012). DOI: 10.1007/s11581-011-0639-y
[5] Yu.S. Akishev, M.E. Grushin, V.B. Karal'nik, A.E. Monich, M.V. Pan'kin, N.I. Trushkin, V.P. Kholodenko, V.A. Chugunov, N.A. Zhirkova, I.A. Irkhina, E.N. Kobzev, Plasma Phys. Rep., **32** (12), 1052 (2006). DOI: 10.1134/S1063780X06120087.
[6] Al.F. Gaisin, F.M. Gaisin, V.S. Zheltukhin, E.E. Son, Plasma Phys. Rep., **48** (1), 48 (2022). DOI: 10.1134/S1063780X22010068.
[7] Al.F. Gaisin, E.E. Son, S.Yu. Petryakov, Plasma Phys. Rep., **43** (7), 741 (2017). DOI: 10.1134/S1063780X17070054.
[8] Yu.P. Raizer, J.E. Allen, V.I. Kisin, *Gas discharge physics* (Springer, Berlin, 1997).
[9] B.Z. Katsenelenbaum, *Vysokochastotnaya elektrodinamika. Osnovy matematicheskogo apparata* (Nauka, M., 1966) (in Russian).

[10] G.I. Skanavi, *Fizika dielektrikov. Oblast' sil'nykh polei* (Fizmatgiz, M., 1958) (in Russian).
[11] A.F. Gaisin, N.F. Kashapov, D.N. Mirkhanov, A.I. Gaisina, A.V. Korneev, in *Nizkotemperaturnaya plazma v protsessakh naneseniya funktsional'nykh pokrytii* (Izd. Kazan. Univ., Kazan, 2019), p. 109 (in Russian).
[12] A.I. Zhakin, Phys.-Usp., **56** (2), 141 (2013). DOI: 10.3367/UFNr.0183.201302c.0153 [A.I. Zhakin, Phys. Usp., **56** (2), 141 (2013). DOI: 10.3367/UFNe.0183.201302c.0153].